FLUTTER SUPPRESSION AND GUST ALLEVIATION USING ACTIVE CONTROLS - REVIEW OF DEVELOPMENTS AND APPLICATIONS BASED ON THE AERODYNAMIC ENERGY CONCEPT

E. Nissim
Department of Aeronautical Engineering
Technion - Israel Institute of Technology
Haifa, Israel

Abstract

The paper presents the current state-of-the-art of the aerodynamic energy concept. The latest applications of the relaxed energy concept, most of which are as yet unpublished, are also presented in this paper. These applications include the suppression of external-store flutter of three different configurations of the YF-17 flutter model, using single trailing-edge (T.E.) control surface activated by single, fixed gain, control law. Also included are some initial results regarding the suppression of flutter of the 1/20 scale, low speed wind-tunnel model, of the Boeing 2707-300 supersonic transport, using an activated T.E. control surface. Additional results regarding comparative study between activated leading-edge - T.E. and T.E. alone control systems are also presented together with a review of previously published formulations and applications.

Introduction

The ability of the aerodynamic control surfaces to promote flutter instabilities has been known for many decades. Classical books in the field of Aeroelasticity[1] include considerable material to this effect under such headings as "bending-aileron flutter" or "torsion-aileron flutter". These control surface induced flutter instabilities are traditionally overcome by reducing the deflections of the control surfaces by mass balancing of the control surfaces. It seems therefore reasonable to assume that this ability of the aerodynamic control surfaces to promote flutter could be reversed by appropriate control of their deflection, so as to combat the main lifting surface flutter instability, such as the wing bending-torsion flutter. Indeed, to put it differently, the origin of flutter lies in the nature of the oscillatory aerodynamic forces which permit the transfer of energy from the airstream to the wing. This flow of energy could be controlled, in principle, by modifying the aerodynamic forces through appropriate deflections of the control surfaces. The implementation of this approach requires, therefore, a rapidly responding control system which is actuated by the motion of the main surface and which leads to an appropriate deflection of the control surface.

The introduction of such activated control surfaces is not limited to problems of flutter suppression. Their potential applications span over a wide class of problems related to the improvement of performance of aircraft. The recent technological advances made in the field of control systems and the increased reliability of control system components, brought about by the space program, have paved the way for the incorporation of increasingly sophisticated control systems in aircraft. In his AIAA Von Karman Lecture[2], I.E. Garruck states: "A major current trend which will play a dominant role in research, development, and practice during the years ahead is the union of modern control technology and aeroelasticity; for example, in control configured vehicles (CCV)... Although aeroelasticians and control specialists have in the past usually gone their separate ways and both fields have become quite sophisticated, in the last few years there have been attempts at real cooperation and adaptation to each other's methods so that important information has been published." Among the numerous proposed applications in CCV are: relaxed aerodynamic stability, gust and maneuver load allevation (with fatigue damage reduction through modal suppression), ride quality control, flutter suppression, taxi load alleviation and automatic control of variable geometry. As could be expected some of the proposed applications have recently come to fruition: An active control system has been installed on the B-52 aircraft[3,4] to control the response of the rigid body mode and one elastic mode (first aft body bending) to gust inputs. Flutter suppression by active controls has been demonstrated in flight[5] on the B-52 airplane (the mild flutter instability was induced by an added ballast tank). Other applications relating to the control of the rigid body modes have been incorporated in several military development areas, including the YF-16 aircraft. Applications relating to the suppression of external store flutter are currently under way for the F4 airplane.[6,7] In addition, a number of feasibility studies have been made to assess the merits (in terms of weight saving and of performance increase) of applications of active control technology to aircraft[8-13] Some of these studies were supplemented by comprehensive wind-tunnel validation programs.[14,15]

As can be seen, the use of active controls spans a wide class of problems. However, one of the major difficulties which characterizes the introduction of active control systems into elastic structures lies in the tendency of the activated systems to be very sensitive to system changes caused by the different flight conditions (such as flight speed, flight altitude, flight duration and type of mission). This sensitivity implies that a control system which is optimized at one flight condition may either show consierable degradation, or even give rise to adverse effects at other flight conditions.

The aerodynamic energy concept was formulated[16] in an attempt to define active control systems which do not exhibit such sensitivities to changing flight conditions. There is no intention to present herein a review of the extensive literature in the field of active control of aeroelastic response, nor is there any intention to review the different approaches and methods available for synthesis. Attempt will only be made in the present paper to review the developments of the aerodynamic

energy approach, together with its applications, to problems of flutter suppression and gust alleviation (with emphasis on flutter suppression problems). Whenver possible, comparisons will be made between results obtained by the aerodynamic energy method and those obtained by other methods such as classical or modern control theory.

The Aerodynamic Energy Approach

Basic Concept

The aerodynamic energy concept was developed primarily for problems of flutter suppression using active controls. It hinges on the idea that since flutter instabilities originate from the nature of the aerodynamic forces, the roots of their suppression should clearly lie in the ability to modify these forces. The above idea can be implemented provided the following problem can successfully be treated: Given a fluttering system and given a control surface which can be activated, what should be the relationship between the oscillation of the system and the deflection of the control surface (normally referred to as "control law") that will ensure the necessary changes in the aerodynamic forces. This problem has been treated in refs. 16, 17. Major points relating to analysis and results are presented in the following section

The Energy Analysis

Let the n equations

$$\{F\} = -\omega^2 [B + \pi\rho b^4 s(A_R + i A_I)]\{q\}+[E]\{q\} \quad (1)$$

represent the equations of motion of n structural modes with r activated controls, where at flutter

$$\{F\} = 0$$

and where ω represents the frequency of oscillation; $[B]$, the mass matrix; $[A_R]$ and $[A_I]$, the real and imaginary parts of the aerodynamic matrix, respectively; $[E]$, the stiffness matrix; ρ, the density of the fluid; s, reference length; b, a reference semichord length; and $\{q\}$, the response vector. The matrices in equation (1) can be partitioned into square matrices ($n \times n$) relating to the structural modes (subscripted by s) and rectangular matrices ($n \times r$) relating to control surface couplings (subscripted by c). After partitioning the matrices, equation (1) becomes

$$\{F\} = \left\{-\omega^2\left[[B_s\,|\,B_c]+\pi\rho b^4 s([A_{R,s}\,|\,A_{R,c}] + i[A_{I,s}\,|\,A_{I,c}])\right] + [E_s\,|\,E_c]\right\}\begin{Bmatrix} q \\ q_c \end{Bmatrix} \quad (2)$$

Assume a control law of the form

$$\{q_c\} = [T]\{q\} \quad (3)$$

where $[T]$ is a ($r \times n$) matrix representing the transfer functions of the control law, and assume that no elastic couplings exist between structural modes and control deflections, thus causing $[E_c]=0$. It can be shown[16,17] that the work P done by the system on its surrounding per cycle can be written as

$$P = \frac{\pi^2\rho b^4 s\omega^2}{2}\lfloor q_R - iq_I\rfloor\,[U]\,\{q_R + iq_I\} \quad (4)$$

where

$$[U] = -\Big([A_{I,s}]+[A_{I,s}]^T+[A_{I,c}][T]+[T^*]^T[A_{I,c}]^T\Big) + i\Big([A_{R,s}]-[A_{R,s}]^T+[A_{R,c}][T]-[T^*]^T[A_{R,c}]^T + \frac{[B_c]\,[T] - [T^*]^T\,[B_c]^T}{\pi\rho b^4 s}\Big) \quad (5)$$

and where

$$\{q\} = \{q_o\}e^{i\omega t} = \{q_R + iq_I\}e^{i\omega t} \quad (6)$$

The sign of P determines stability, and therefore it is advantageous to convert equation (4) to a more convenient form. It can be shown[16,17] that P can be reduced to the form

$$P = \tfrac{1}{2}\pi^2\rho b^4\omega^2 s\Big(\lfloor\xi_R\rfloor\,[\lambda]\{\xi_R\} + \lfloor\xi_I\rfloor[\lambda]\{\xi_I\}\Big) \quad (7)$$

or alternatively

$$P = \tfrac{1}{2}\pi^2\rho b^4\omega^2 s\left[\lambda_1\left(\xi^2_{R,1}+\xi^2_{I,1}\right) + \lambda_2\left(\xi^2_{R,1}+\xi^2_{I,2}\right) + \ldots + \lambda_n\left(\xi^2_{R,n} + \xi^2_{I,n}\right)\right] \quad (8)$$

where $[\lambda]$ is a diagonal matrix of the eigenvalues λ_i necessarily real, of the Hermitian matrix $[U]$ (as given by eqn (5)), and where the vectors $\{\xi_R\}$ and $\{\xi_I\}$ are defined by the transformation

$$\{q_o\} = [Q_R + iQ_I]\,\{\xi_R + i\xi_I\} \quad (9)$$

The matrix $[Q_R + iQ_I]$ is a square modal matrix of the principal eigenvectors.

Discussion of Energy Concept

The work per cycle P done by the system on its surroundings has a direct bearing on the stability of the system. If P is positive, the system is dissipative, and therefore stable. If P is negative, the system is unstable because work is done by the surroundings on the system. Equation (8) shows that if all the eigenvalues λ_i of the system are positive, the system is stable regardless of the motions represented by the generalized energy coordinates ξ. If one or more of the λ eigenvalues is negative, the system is potentially unstable. Its ultimate stability is determined by the relative values of the terms ξ and λ. If the ξ values make the positive eigenvalues dominate the right-hand side of equation (8), the work P is positive and the system is stable. If, on the other hand, the ξ values make the negative terms dominate eqn. (8), P is negative and the system is unstable. Hence, the requirement for all λ's to be positive is a sufficient but not a necessary condition for stability.

For mass-balanced control surfaces ($[B_c]=0$, the eigenvalues λ obtained from $[U]$ (Eq. (5)) are dependent only on the aerodynamic properties of the system and the activated control law (matrix $[T]$). In the case of mass-balanced surfaces, the eigenvalues are referred to as aerodynamic eigenvalues. These latter eigenvalues are, in general, functions of the reduced frequency k and Mach number M. If mass unbalance is a fixed quantity in the system, the eigenvalues λ also depend on the fluid density ρ in addition to their dependence on k and M. Note that instability at zero airspeed can be brought about only through these mass unbalance

terms. All the results presented in this paper relate to mass-balanced control systems only and therefore, aerodynamic eigenvalues are obtained from the following [U] matrix

$$[U] = -\left([A_{I,s}]+[A_{I,s}]^T+[A_{I,s}][T]+[T^*][A_{I,c}]^T\right)$$

$$+ i\left([A_{R,s}]-[A_{R,s}]^T+[A_{R,c}][T]-[T^*]^T[A_{R,c}]^T\right) \quad (10)$$

It may be recalled that the energy approach, in its original development[16], sought to determine the matrix [T] to render all the aerodynamic eigenvalues (of matrix [U] eq. (10)) large and positive. This requirement regarding the aerodynamic eigenvalues insures both the stability of the system (since P is always positive) and its insensitivity to various flight conditions (which manifest themselves in the form of changing values of λ and changing values of the system responses ξ).

Generalized Model

The energy approach has been formulated for a general n degree of freedom system. Therefore, the energy concept can be applied to any problem. The results of such application, however, will be specific for the system considered since the generalized aerodynamic forces depend not only on the system geometry but also on its structural natural modal responses. If, however, the energy concept is applied to a two dimensional strip, the aerodynamic matrices are independent of geometry and responses of the system. As a result, the aerodynamic eigenvalues are independent of any specific system and are only functions of k, M, and the transfer function matrix [T]. Therefore, if [T] is defined using a two-dimensional strip as a model, these [T] values are applicable to any three-dimensional wing within the limitations of strip theory; thus, the model is generally applicable. Sketch (a) illustrates the generalized model considered, and the arrows indicate positive displacements and rotations.

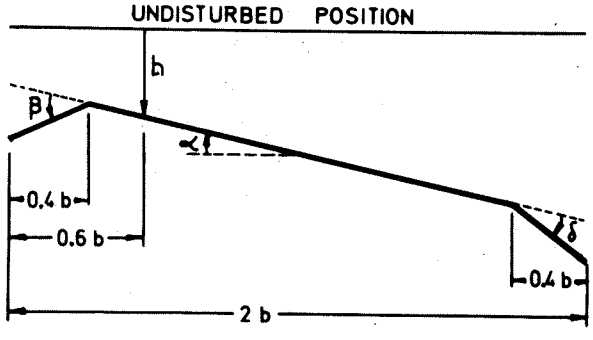

Sketch (a)

Analysis of the Generalized Model

The motion of the generalized two-dimensional model is defined by two parameters: the displacement h of the 30 per cent chord point and the rotation α about this point. Two control surfaces are assumed to be available for activation: a 20 per cent chord trailing-edge (T.E.) control and a 20 per cent chord leading-edge (L.E.) control. Two aerodynamic eigenvalues, λ_{min} and λ_{max} are obtained using this model. The analysis and results which accompanied the original derivation of the energy concept,[16] employed a transfer function matrix of the form

$$[T] = [C] + i\,[G] \quad (11)$$

The matrices [C] and [G] were assumed to have constant values (in eqn (11)) thus making the subsequent mechanization of the control law difficult. The matrix [T] was determined numerically by an optimization program which required λ_{min} to be positive and large over a wide range of k values. This was achieved by maximizing the area under the curve λ_{min} vs 1/k using the C_{ij} and G_{ij} terms as parameters.

It should be stressed at this stage that the generalized two-dimensional model adopted herein serves only to indicate, on the basis of the strip theory, whether energy is dissipated or absorbed by the partial span strip where the activated controls are installed. Therefore, in order to suppress flutter with a minimum number of activated partial span strips, one should aim at dissipating enough energy in the activated strip, so as to compensate for any energy input by the nonactivated portions of the wing. One should therefore attempt not only to turn λ_{min} positive but also to cause λ_{min} to assume large (and positive) values.

Results of the Original Formulation of the Energy Concept

Typical results obtained with M=0 using the procedure just described[16] are presented in Fig. 1 for the unactivated system, in Fig. 2 for the activated T.E. control and in Fig. 3 for the activated combined L.E.-T.E. control system (for further details see ref. 16). The optimized values of the transfer functions [C] and [G] for these two types of activated systems are given by

a) For the T.E. Control system

$$[C]_{opt} = \begin{bmatrix} 0 & 0 \\ -0.35 & -1.9 \end{bmatrix}; \quad [G]_{opt} = \begin{bmatrix} 0 & 0 \\ 0.35 & 0.1 \end{bmatrix} \quad (11a)$$

b) For the combined L.E.-T.E. Control system

$$[C]_{opt} = \begin{bmatrix} 0.5 & 1.0 \\ -0.05 & -1.7 \end{bmatrix}; \quad [G]_{opt} = \begin{bmatrix} -0.5 & 1.0 \\ 0.45 & 0.2 \end{bmatrix} \quad (11b)$$

The following points emerging from these figures are worth noting:

1) The value of λ_{min} for the inactivated system (fig. 1) is negative throughout the range of k ($0.0128 \leq k \leq 19.5$) and the value of λ_{max} is positive throughout this same range. Furthermore, the absolute values of $|\lambda_{min}|$ and $|\lambda_{max}|$ are of the same order of magnitude.

2) The values of λ_{min} for the T.E. system (Fig. 2) is only marginally positive (except at high k values) and is highly sensitive to off-design values. The values of C_{22} which improve λ_{min} cause λ_{max} to deteriorate appreciably.

3) The optimum values of λ_{min} for the combined L.E.-T.E. control system (Fig. 3) is large and positive over the whole range of 1/k. The off-design sensitivity is greatly reduced as compared with the T.E. control system. Here again, the values of C_{22} which improve λ_{min} cause λ_{max} to deteriorate.

The results presented in ref. 16 indicate the following additional important points:

4) Systems having two sensors (to determine both h and α) are superior to any single-sensor system.

5) Mach number effects are beneficial for the whole k range for the L.E.-T.E. system (fig. 4) whereas the T.E. system shows minor improvements except for the very low range of k values where some deterioration takes place.

6) The values of λ_{min} (and λ_{max}) for the L.E.-T.E. control system could be increased considerably by the simultaneous increase of all the G_{ij} terms by a constant factor $\omega/\omega_r>1$ (see fig. 5). The T.E. control system showed a deterioration in λ_{min} accompanied by a considerable improvement in λ_{max} when such an increase in its G_{ij} terms was attempted (see ref. 16). Thus, the control law for the L.E.-T.E. system could be brought to the following convenient form

$$\{\beta\} = [C] \begin{Bmatrix} h/b \\ \alpha \end{Bmatrix} + \frac{1}{\omega_r} [G] \begin{Bmatrix} \dot{h}/b \\ \dot{\alpha} \end{Bmatrix} \qquad (12)$$

where ω_r is a reference frequency which maintains the non-dimensional nature of eqn. (12). Clearly, the mechanization of this latter control law is much simpler than the one given by eqn. (11).

The above results led to the conclusion that the L.E.-T.E. control system, driven by two sensors, is the most effective system for purposes of flutter suppression. For this reason the L.E.-T.E. system was chosen for testing the effectiveness of active controls in the early applications of the energy method. However, before proceeding to these applications, a few points should be mentioned regarding the physical significance of the optimized control laws (see sketches (b) and (c)). The optimized L.E.-T.E. control law will be chosen for this

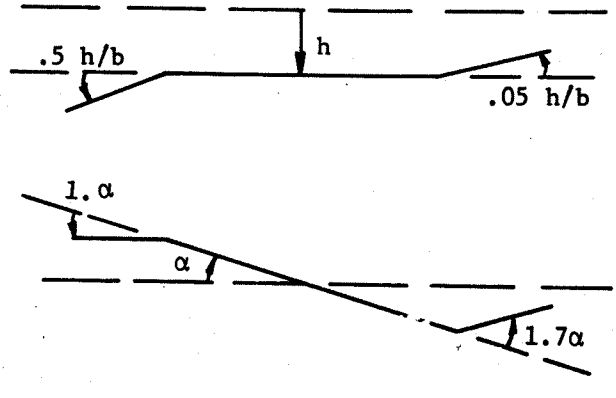

Sketch (b)

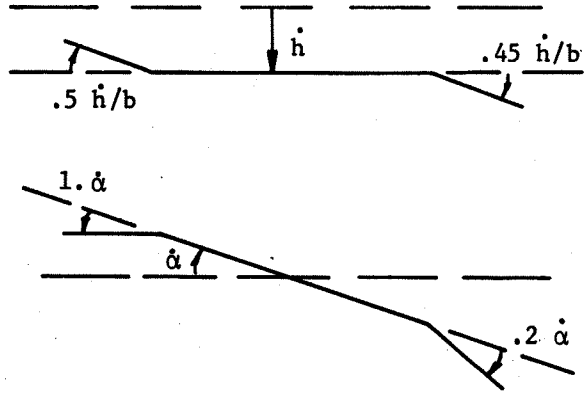

Sketch (c)

purpose since it includes the essential features of the two control surfaces employed by the generalized model.

It is interesting to note that the main effect of the in-phase deflections of the control surfaces is to counteract any lift building up; that is, the lift increase due to the angle of attack α is opposed by the forces created by the deflections of the L.E. and T.E. control surfaces. Furthermore, the out-of-phase control deflections increase the damping forces. It can therefore be seen that flutter suppression is achieved by both reducing the energy input into the system and increasing the dissipation of energy.

Early Applications of the Aerodynamic Energy Concept

The first application of the results produced by the aerodynamic energy concept was made using a SST type wing for which detailed analysis using at least 10 degress of freedom already existed[18]. The application was carried out by members of the Boeing Wichita division under contract to the Langley Research Center. The wing configuration is indicated in Fig. 6. Flutter control was achieved using several independent stripwise units each of which consisted of combined L.E.-T.E. control surfaces having 20% chord each and activated by sensors located at 30% and 70% chord locations, (using a control law as given by eqn (11)). The results, employing M=0.9 lifting surface aerodynamics, supplemented by strip theory for the control strips, indicated that the use of T.E. controls alone would increase the flutter speed by only a few per cent ($\sim$ 5%) while the use of the combined L.E.-T.E. systems yielded with outboard segment A alone an 11% increase, with mid segment B alone - 28% increase, and with inboard segment C alone - 21% increase in the flutter speed. The combined use of B and C led to an increase in flutter speed not specifically determined but noted to be in excess of 41% of the original speed. A root locus plot corresponding to this case is shown in Fig. 7. A corresponding experimental exploratory study[15] was undertaken in the Langley Transonic Dynamics Tunnel using a simplified version of a proposed supersonic transport wing design (Fig. 8). The active flutter suppression method, based on the aerodynamic energy criterion, was verified experimentally using three different control laws (as defined by eqn (11)). The first two control laws utilized both leading edge and trailing-edge active control surfaces, whereas the third control law required only a single

T.E. control surface. At Mach number 0.9 the experimental results demonstrated increases in flutter dynamic pressure from 12.5 per cent with a L.E.-T.E. active control system to 30 per cent with active T.E. control. The mechanization of the L.E. control has met with great difficulties due to what is now believed to be a control induced instability caused by the mass unbalanced L.E. control. As a result of this instability of the L.E. control (which was present even at zero airspeeds) activation of the L.E. control could only be attained at M=0.9. Nevertheless, two important points follow this essentially experimental study (15).

1) An active flutter suppression system was demonstrated successfully, using L.E. and T.E. control surfaces, to suppress flutter on a model in a wind tunnel.

2) Irrespective of the difficulties encountered in the mechanization of the L.E. control, it is still significant to note that a single T.E. control yielded satisfactory results in suppressing flutter over the entire range of Mach numbers tested.

Somewhat different analytical applications (19,20) using a somewhat different control law, of the type given by eqn (12), with ω_r acting as a control parameter (the smaller ω_r is, the more effective the active controls become), were made on two different types of subsonic aircraft using a discrete gust approach (20) based on aerodynamic strip theory. These aircraft are the twin-boom, twin-turboprop Arava STOL transport (maximum mass 6800 Kg, see Fig. 9) and the Westwind, twinjet business transport (maximum mass 9400 Kg) which is a modified version of the Rockwell Jet Commander (Fig. 10). The wing on each aircraft was divided into 10 equally spaced strips as shown in Fig. 11: Each strip could accommodate a pair of active controls (that is, 20% chord L.E.-T.E. controls). The strips located along the horizontal tail were allowed spans equal to one third and one tenth of the horizontal tail semispan of the Arava and Westwind aircraft respectively. The best locations for a single activated system along the span of the wing were determined for bending-moment alleviation, reduction in fuselage accelerations, and flutter suppression. Reference 19 deals with step gust inputs whereas reference 20 deals with 1-cos shape gust with peak values following the requirements of the federal aviation authorities.

The simultaneous treatment of flutter suppression and gust alleviation problems follows as a natural consequence of the control law derived by the use of the aerodynamic energy which, as already mentioned earlier, acts to reduce the energy input into the system and increase the dissipation of energy.

The main points emerging from this application (20) are briefly summarized by the following points:-

1) A single activated strip located at the outboard region of the wing promotes negative bending moments (M_b) at the root of the wing during upgust conditions (see Fig. 12). These negative bending moments are caused by the restraining forces exerted by the activated strip, at its outboard location, as a result of the upward motion of the airplane caused by the upgust forces. For similar reasons, an activated strip located at the root region of the wing promotes increase in bending moments during upgust conditions (see Fig. 13).

   To overcome these difficulties, the control law was modified to activate the control surfaces using the elastic contributions of the motion. In mathematical terms, h and α in the control law were replaced by $(h-h_r)$ and $(\alpha-\alpha_r)$ where the subscript r refers to a reference point around the root of the wing. This reference point is chosen in such a manner so as to "filter out" all the rigid body contributions to the control inputs. The results following the introduction of the above changes into the control law (referred to in ref. 20 as the extended control law) are shown in Fig. 14. As can be noted, the effects of the extended control law on the maximum values of the root bending moment are indeed dramatic. The best location of the activated strip for maximum bending-moment reductions is in the tip region of the wing but inboard of the tip strip.

2) The optimum strip location for maximum increase in the flutter speed is at the wing tip strip. Furthermore, the effectiveness of the activated strip is greatly increased by the introduction of the extended control law. Flutter speeds could easily be increased by more than 70% of the open loop flutter speeds.

3) The optimum strip location for maximum reductions in fuselage accelerations is at the root strip location for the ordinary control law (Fig. 15). The extended control law yields better results with optimum strip location at the inboard region of the wing (but clearly not on the reference strip, see Fig. 16).

In summarizing the results of the above application (20), it may be stated that the extended control law, which is based on the wing elastic deformations only, presents a major step forward in problems of flutter suppression and gust alleviation. It leads to almost complete decoupling between the rigid-body responses, elastic responses, and the activated control forces. As a result, major improvements in performance are obtained. For this reason, free flying wind tunnel models might show greatly reduced performance as compared with clamped models unless some form of an extended control law is used.

The above applications have shown that the energy concept produces effective activated systems. There were indications, however, that the derived control laws could be improved and that the mechanization of the L.E. control was more involved than that of the T.E. control. Furthermore, some of the control laws (such as the one defined by eqn (11)) were difficult to realize. This led to an investigation aimed at avoiding the use of the L.E. control while maintaining the effectiveness of the activated system. The results of this investigation are described in the following section.

Active Flutter Suppression Using Trailing-Edge and Tab Control Surfaces

As already stated earlier in this paper, the L.E. control may present some control problems since it carries relatively large aerodynamic hinge moments. Furthermore, there has been some reluctance to introduce a L.E. control due to its possible detrimental effects on the general aerodynamic characteristics of the wing. The activated T.E.-tab combination, if effective for flutter suppression, could alleviate the difficulties associated with the L.E.-T.E. system. It is shown [21] that an 8% chord tab should be chosen for a 20% chord T.E. control. The results obtained [21] for the variations of λ_{min} with $1/k$ show that the T.E.-tab system activated by both linear and rotational sensors, has a flutter suppression performance comparable to the L.E.-T.E. system. The main advantage of the T.E.-tab system over the L.E.-T.E. system lies in the lower actuator torque requirements, whereas its main disadvantage lies in its relatively higher control surface rotations. Applications pertaining to the T.E.-tab system were not further pursued in view of the progress made regarding the activation of T.E. alone control system. Some details regarding these developments are presented in the following section.

Relaxation of the Energy Concept

Objective and Formulation of Relaxed Conditions

The energy approach, in its original development [16], sought to determine the matrix $[T]$ so as to render all the aerodynamic eigenvalues large and positive. This requirement regarding the aerodynamic eigenvalues ensures both the stability of the system (since P will always be positive) and its insensitivity to the various flight conditions. Since the derived control laws are of general nature and do not take into consideration any specific property of the analysed system, it is possible to argue that the limitations concerning the potentials of the T.E. control system to perform effectively as flutter suppressor is inherent in the above formulation of the problem. Assume that other methods of stabilization exist, or can be devised, and that all we wish to ensure is the insensitivity of the stabilized system to changes in flight conditions. The implications of such an approach on the energy concept involve the relaxation of the requirement that all the aerodynamic eigenvalues must be large and positive. Assume, therefore, that such a relaxation is now introduced which permits some of the aerodynamic eigenvalues to be negative. Stability can only be achieved under these conditions by modifying the responses of the system so as to render the responses associated with the positive eigenvalues to be the dominant ones. This latter requirement forms a necessary condition for stability but does not ensure, in itself, the insensitivity of the resulting stabilized system to the various flight conditions. In order to ensure that this relaxed stability requirement yields a system which shows only small sensitivities to the changing flight conditions the absolute values of the negative aerodynamic eigenvalues must always be made much smaller than those eigenvalues associated with the dominant responses of the stabilized system. For the generalized two-dimensional model adopted in this work, two aerodynamic eigenvalues, λ_{min} and λ_{max} are obtained. In the original derivation of the aerodynamic energy concept, λ_{min} was required to be positive and large. In the relaxed energy approach, [17] λ_{min} is permitted to be negative provided

$$\lambda_{min} = \text{near maximum value (may be negative)}$$
$$\lambda_{max} >> \lambda_{min} \qquad (13)$$

and provided that these relations are maintained for all flight conditions. The above two requirements regarding λ_{min} and λ_{max} will be referred to as the "relaxed energy requirements". As can be noted, the above relaxation is made possible by abandoning the sufficiency condition for stability in the original formulation while maintaining its insensitivity to changes in flight conditions. It is worth noting that since the dissipation of energy by the activated strip depends both on λ_{min} and on λ_{max}, the importance of λ_{max} should not be overlooked even when λ_{min} is positive and large. Considerable improvements in the potential performance of the activated control system may result, if changes in the control gains are permitted which lead to small degradations in λ_{min}, provided these degradations are accompanied by large increases in λ_{max}. This implies that while determining the optimum values of the transfer function matrix $[T]$ we seek to optimize not only the area under the λ_{min} vs $1/k$ curve but also the weighted addition of the area under the λ_{max} vs $1/k$ curve, so as to satisfy eqns (13). Convenient ways of performing the above optimization of the $[T]$ matrix are described in ref. 17.

In addition to the above relaxation of the energy concept, two other major changes were introduced in ref. 17:

1) Unlike the original derivation, only realizable transfer functions were considered

2) The influence on the target function of the very low frequency portion of the λ vs $1/k$ curves was reduced by both an appropriate redefinition of the aerodynamic eigenvalues and the reduction of the k range from

$$0.0128 \leq k \leq 19.5$$

as used during the original derivation, [16] to

$$0.04 \leq k \leq 3.5$$

The redefintion of the aerodynamic eigenvalues involves the inclusion of the frequency effects into these aerodynamic eigenvalues. Hence, eqn (8) was modified to the form

$$P = \tfrac{1}{2}\pi^2\rho b^2 V^2 s \left| \bar{\lambda}_1\left(\xi^2_{R,1} + \xi^2_{I,1}\right) + \bar{\lambda}_2\left(\xi^2_{R,2} + \xi^2_{I,2}\right) + \ldots\ldots + \bar{\lambda}_n\left(\xi^2_{R,n} + \xi^2_{I,n}\right) \right| \qquad (14)$$

yielding the following relation between the λ's

$$\bar{\lambda}_i = k^2 \lambda_i \qquad (15)$$

Hence, at the low range of k values, the newly

defined eigenvalues are smaller than the originally defined eigenvalues by a factor of k^2. These changes permit the giving of more weight to the intermediate frequencies during the optimization process.

Optimization Results[17]:

The variation of the non activated $\bar{\lambda}$'s with $1/k$ is shown in Fig. 17. It is interesting to compare these $\bar{\lambda}$ with their λ counterparts in Fig. 1 and to note the large changes in the shape of the curves.

Two types of optimized transfer functions were derived.[17] The first type is referred to as the damping type transfer function (D.T.T.F.) and it assumes the following optimum values for [T].

$$[T] = \begin{bmatrix} 0. & 0. \\ 0. & -1.86 \end{bmatrix} + ik \begin{bmatrix} a_L & 0 \\ 0 & a_T \end{bmatrix} \begin{bmatrix} -4. & 4. \\ 4. & 3.2 \end{bmatrix} \quad (16)$$

where a_L and a_T are positive free parameters. These free parameters were introduced as a result of the unbounded behaviour of the target function with respect to increase of these parameters. The transfer function for the T.E. alone system is obtained from eqn (16) by letting $a_L=0$.

The second type of optimized transfer function is referred to as the localized damping type transfer function (L.D.T.T.F.) and it assumes the following optimum values for [T]

$$[T] = \begin{bmatrix} 0. & 0. \\ 0. & -1.86 \end{bmatrix} + R \begin{bmatrix} a_L & 0 \\ 0 & a_T \end{bmatrix} \begin{bmatrix} -4. & 4. \\ 4. & 2.8 \end{bmatrix} \quad (17)$$

where once again a_L and a_T are positive free parameters (which follow the unbounded nature of the target function with increase of these parameters) and R is given by

$$R = \frac{(ik)^2}{(ik)^2 + 2\zeta k_n (ik) + k_n^2} \quad (18)$$

where both ζ and k_n are positive constants. Fig. 18 shows the variation of $\bar{\lambda}_{min}$ vs $1/k$ and $\bar{\lambda}_{max}$ vs $1/k$ at various Mach numbers using the optimized D.T.T.F., as defined by eqn (16) with $a_L=0$ (that is, T.E. only control system) and $a_T=25$. The corresponding curves using the L.D.T.T.F. defined by eqns (17,18) are shown in Fig. 19 using the values of $a_L=0$, $a_T=1$, $\zeta=0.5$ and $k_n=0.2$. It can be seen that the results corresponding to the D.T.T.F. (Fig. 18) satisfy the relaxed energy requirements (as expressed by eqn (13)) over the whole range of k's investigated. The L.D.T.T.F. yields results (Fig. 19) which satisfy the relaxed energy requirements only around the peak region of the curves. The location of this peak region (along the $1/k$ axis) is around $1/k_n$ and the width of the curves (in addition to their height) are controlled by the parameter ζ. In addition, stiffness terms are introduced as R varies with k. These terms vanish when k=0 and therefore do not affect the static behaviour of the system. They, however, can be used to change the response of of the system, if necessary, so as to ensure stabilization. In general, several R values can be used, having different values of k_n, ζ and a's, if greater flexibility in the $\bar{\lambda}$ distributions (with k) is required while using the L.D.T.T.F. (see ref. 22). For the L.E.-T.E. systems, large improvements in the values of $\bar{\lambda}_{min}$ are obtained (see ref. 17) with almost negligible effects on the values of $\bar{\lambda}_{max}$ (as compared with the T.E. alone control system).

The working forms of the above transfer functions are simplified to the following forms for purposes of subsequent applications:-

For the D.T.T.F. matrix [T] is given by

$$[T] = \begin{bmatrix} 0 & 0 \\ 0 & -1.86 \end{bmatrix} + i\frac{\omega}{\omega_R} \begin{bmatrix} a_L & \\ & a_T \end{bmatrix} \begin{bmatrix} -4. & 4. \\ 4. & 3.2 \end{bmatrix} \quad (19)$$

where ω_R is a reference frequency, normally chosen as the open-loop flutter frequency. For the L.D.T.T.F., matrix [T] is given by

$$[T] = \begin{bmatrix} 0. & 0. \\ 0. & -1.8 \end{bmatrix} +$$

$$+ \begin{bmatrix} (R_{L,1}\, a_{L,1} + R_{L,2}\, a_{L,2}) & 0 \\ 0 & (R_{T,1}\, a_{T,1} + R_{T,2}\, a_{T,2}) \end{bmatrix} \cdot$$

$$\cdot \begin{bmatrix} -4. & 4. \\ 4. & 2.8 \end{bmatrix} \quad (20)$$

where

$$R_j = \frac{(i\omega)^2}{(i\omega)^2 + 2\zeta_j \omega_{n,j} (i\omega) + (\omega_{n,j})^2} \quad (21)$$

It can be seen that both transfer functions include parameters which can only be determined in connection with the system considered. The L.D.T.T.F. has more parameters for determination and has more potential regarding possible changes in the responses of the system. It is generally considered to be preferable to the D.T.T.F. On the other hand, the D.T.T.F. has less such parameters and, therefore, their values are much easier to determine.

Analytical Applications of the Relaxed Energy Approach

An optimization procedure was developed[22] for the determination of the various free parameters (that exist in the above transfer functions) so as to minimize control surface response to continuous gust inputs over a wide range of flight conditions. Most applications relate to T.E. alone control systems in an attempt to determine their effectiveness for flutter suppression. Extended type control laws (driven by the elastic responses of the system) were exclusively employed in all applications.

The first application of the above optimization procedure using the newly defined transfer functions was made to a violent wing flutter case of a drone aircraft[29] selected by the National Aeronautics and Space Administration for flight research programs aimed at validating active control

system concepts. A plan view drawing of the flight vehicle-research wing combination is shown in Fig. 20. Guided by previous results[20], the T.E. control surface was placed as near to the tip of each wing as was structurally possible (Fig. 21). All the aerodynamic forces were computed using unsteady lifting surface doublet lattice method. The design objective of the flutter suppression system was to provide a 20% increase in flutter speed (to be demonstrated in flight) above that of the basic wing. Although detailed results regarding this case appear in ref. 22, preference will be given here to the results appearing in ref. 23 since they include comparisons with results obtained using classical control system synthesis. Table 1 presents a summary of the calculated flutter characteristics. It can be seen that both the classical and the energy methods achieve the objective set for the flutter suppression system (with somewhat higher flutter speed values using the energy method). Figure 22 shows comparisons of control surface rates and displacements. As can be seen, the maximum values for the rates (and displacements) using the energy method are around 20% lower than those produced by the classical method. In their discussion of results the authors state [23]: "Two major differences result in the application of these methods. The first difference is in establishing the form, gains, and break frequencies of the shaping filter. In the classical method, this process is a function of previous experience coupled with results of analysis for the particular system being studied and in general cannot be extended to other problems. In the aerodynamic energy method, on the other hand, a fixed form of the shaping filter is given with free parameters available to fit this form to the dynamic characteristics of the system being considered. The second difference is the manner in which the gust analysis is used. In the classical method the gust is used to evaluate rates and deflections of the control system after preliminary design of the shaping filter is complete. If the rates or deflections are beyond the capability of the control system then an iterative process including changes to the shaping filter and possibly the control surface size is begun. This process is continued until both the stability and gust response requirements are met. In the energy method, the fixed form of the shaping filter allows the gust to act as a driver in establishing the free parameters which in turn permits the minimization of control surface activity while maintaining stability."

A second application has recently been made to the YF-17 flutter model[24] with the object of suppressing the external store flutter of three different store configurations using a T.E. alone control surface. The geometrical description of the active control system is shown in Fig. 23. Note that the T.E. control surface spans only 7 per cent of each wing. The description of the three configurations is given in Table 2 and the results of the optimization procedure are given in Table 3. These latter results relate to M=0 and V=98 m/s and were obtained using a dynamic pressure Q_D which is twice the value (determined arbitrarily in the absence of a definition of the desired flight envelope) of the minimum flutter dynamic pressure, corresponding to configuration B. A L.D.T.T.F. was employed and its free parameters were determined using configuration B. The resulting control law was maintained fixed during applications to configurations A and C. The significance of these results is threefold:

1) A single control law with fixed gains is employed for all configurations

2) Very large increases in flutter dynamic pressures are obtained for all configurations

3) The effectiveness of the activated control system is maintained over the whole range of flight conditions (thus providing yet another confirmation regarding the potential of the relaxed energy concept).

It may also be worth noting that although the open loop configruation B is most critical from flutter considerations, the largest control surface activity corresponds to configuration C. This activity can be reduced by increasing the span of the control surface ($\sim$ 7%) employed in this application.

A single application of a L.E.-T.E. control system has recently been made using the previously described drone aircraft.[25] It is shown that the L.E.-T.E. control system yields a closed loop system with flutter speeds which are higher than those of the T.E. alone system. In addition the activity of each of the control surfaces in the L.E.-T.E. system is much lower than that corresponding to the T.E. alone system. If, however, the performance of the two systems is judged on the basis of the maximum control surface activity (corresponding to the desired 44% increase in the flutter dynamic pressure) rather than on the maximum flutter speed, and if we further require that the performance of a system with two control surfaces be compared only with systems having two control surfaces (in this case a comparison between L.E.-T.E. and T.E.-T.E. systems) one finds that the performance of the L.E.-T.E. control system is comparable to the performance of the T.E. alone system, with slight advantage to the latter system. Although this finding may be of specific nature and need not necessarily hold true for other applications, it is of importance since it shows that a T.E. alone control system can yield results which compare favourably with a L.E.-T.E. control system.

It is not unintentional that we choose to close the circle of applications by returning to the first example which served to test the potentials of the aerodynamic energy method - that is the application relating to the Boeing's supersonic transport. Comparison is now made between the results reported in reference 26, and which forms Phase II of the SST technology follow-on program, and those obtained through the use of the relaxed energy concept.[27] These results relate to the full span 1/20 scale low-speed model of the Boeing 2707-300 supersonic transport. Figure 24 shows the general configuration of the model. It can be seen that two T.E. control surfaces are available for activation. The application based on classical control methods[26] attempted the activation of both control surfaces whereas the application based on the energy approach [27] attempted the activation of the outboard aileron only (based on experience gained from previous applications[20]). These results, which were obtained using lifting surface unsteady aerodynamics, are presented in Fig. 25. As can be seen, the energy method yeilds an increase in flutter speed

of 33% using the outboard aileron only (and L.D.T.T.F.) whereas the classical method yields an increase in flutter speed of 11.3% only, using both outboard and inboard ailerons. Furthermore, the energy method yields the following control surface activity of the outboard aileron, at a speed which is 16% above the inactivated flutter speed

$$\dot{\delta}_{RMS} = 25.3 \text{ deg/s/m/s}$$

$$\delta_{RMS} = 0.33 \text{ deg/m/s}$$

These activities are not considered to be excessive. It should be noted that flutter speeds could further be increased by specifying higher flight dynamic pressures when using the gust optimization program.

Remarks on Applications using Modern Control Theory

The author of this paper is unaware of any major comparative studies between designs based on the aerodynamic energy method and those based on modern control theory. Some use has, however, been made of the aerodynamic energy control law (eqns (11b), (12)) as derived for the L.E.-T.E. system in the original formulation of the energy concept in connection with some work which employed optimal control methods[28]. The above control law was applied[28] to a two dimensional subsonic strip, with specified actuator dynamics included in the analysis. The results showed that the plunge and pitch modes were stabilized throughout the range of parameters investigated whereas the leading-edge control mode was unstable throughout this range. Such a condition can arise if one considers the control laws of the form given by eqn (3) to correspond to the command deflections rather than to the actual deflections. It should therefore be stressed that control surface dynamics should be compensated in all applications employing the energy control laws so as to cause the transfer function matrix [T] to relate between the structural oscillations and the actual control surface deflections. It is worth mentioning the results which correspond to the above mentioned two dimensional strip as obtained through the use of optimal control theory [28]. It will be appropriate, however, to make a brief introduction to the method used.

The linear optimal control theory requires[29] the equations of motion of the system to be brought to the following form

$$\{\dot{X}\} = [A]\{X\} + [B]\{u\} \qquad (22)$$

where $\{X\}$ represents the N state variables, $[A]$ (of order N x N) the plant (or system) matrix; $[B]$ (of order N x m) the control distribution matrix; and $\{u\}$ (of order m) the control input vector. Both the matrices $[A]$ and $[B]$ (eqn 22) are constant for a given Mach number, given flight velocity and given flight altitude. Optimal control theory requires the minimization of the performance index (PI), with equations (22) used as constraints, where PI is given by

$$PI = \int_0^\infty \left(\lfloor X \rfloor [Q]\{X\} + \lfloor u \rfloor [P]\{u\} \right) dt \qquad (23)$$

and where $[Q]$ is either positive definite or positive semidefinite, and $[P]$ is always required to be positive definite. The problem now remains of selecting the weighting matrices $[Q]$ and $[P]$. For the minimization of $\{u\}$, $[Q]$ is chosen as $[Q]=0$. The resulting optimized control law, which is of the form

$$\{u\} = [T]\{X\} \qquad (24)$$

where the T_{ij} terms are constants, causes all the stable open-loop eigenvalues to remain unchanged while the open-loop unstable eigenvalues are reflected about the $i\omega$ axis (that is, the sign of the real part of the unstable roots is reversed). This result (see also ref. 31) permits application of the "pole placement" method for the determination of the matrix $[T]$. Application of the above optimal control method was made to the two dimensional strip example using a T.E. only control system[28]. The stabilized closed-loop system was found to become unstable below the open loop flutter speed, thus showing the importance of the sensitivity of the activated system to off-design conditions. The above system with two control surfaces was eventually stabilized by reflecting the unstable flutter eigenvalue about a line parallel to the $i\omega$ axis and crossing the real axis of the root locus plot at a value of 5 rads/sec. Such a reflection is arbitrary and is not, in itself, a result of application of optimal control considerations. It can thus be seen that off-design considerations forces the designer to compromise for a suboptimal system. The aerodynamic energy concept introduces these compromises in a consistent manner whereas other methods deal with this problem in an ad hoc arbitrary fashion.

An additional point which is worth noting relates to the inclusion of the actuator dynamics in the plant equations (22). It is felt that such inclusion[28,30] is limiting since parameters relating to control surface dynamics can be changed if necessary so as to reduce control surface activity. The exclusion of control surface dynamics from the energy synthesis considerations should therefore be viewed as promoting efficiency rather than as a limitation. The form of the various R's (eqn (18)) associated with the L.D.T.T.F. have the form of an actuator transfer function. It is therefore possible to view the values of the optimized R's as representing the desired actuator dynamics. These latter values clearly indicate the changes that need to be introduced into the existing actuator.

As a final remark, it is interesting to note that the determination of the control law using the energy concept meets none of the difficulties which characterize the optimal control approach such as problems associated with aerodynamic modeling, state augmentation and eventually, the state vector identification for purposes of implementation of the control law. The use of the continuous gust program for the minimization of the control surface activity using the energy method presents absolutely no aerodynamic modeling or state augmentation problems. Similarly, the relationship between the control surface deflection and the response of the wing at a specified location (see eqn (12) as an example) presents no need for state vector identification (this is similar to the I.L.A.F. concept developed in reference 8).

Concluding Remarks

The paper presents the current state-of-the-art

of the aerodynamic energy concept. Many of the applications relating to the relaxed energy method have not yet been published. It is felt that the relaxed energy method, coupled with the gust response optimization procedure yields effective control systems for the suppression of flutter. These systems may consist of either L.E.-T.E. or T.E. alone control surfaces. These activated systems may also be used for gust load alleviation and ride control (if appropriately located) as shown in one of the early applications. There remains to extend the method to the supersonic flight regime and to test the possible advantages of deriving control laws based on the system's generalized matrices (somewhat along the lines of ref. (31) using the relaxed energy approach) rather than on the generalized two-dimensional strip model.

Further substantiation of results is needed using both wind tunnel models and flight test programs before attempting to incorporate some flutter suppression systems in either existing or future aircraft.

Acknowledgement

All the work performed by the author in the field of active controls was supported by NASA-Langley Research Center, through grants and through NRC Research Associateships. The author wishes to express his sincere thanks and appreciation for this support and for the continued encouragement given by the NASA (Langley) Aeroelasticity Branch throughout the years.

References

1. Bisplinghoff, R.L., Ashley, H. and Halfman, R.L.: Aeroelasticity, Addison-Wesley Publishing Co., 1955.

2. Garrick, I.E.: Aeroelasticity - Frontiers and Beyond. J. Aircraft, September 1976.

3. Dempster, J.B. and Roger, K.L.: Evaluation of B-52 Structural Response to Random Turbulence with Stability Augmentation Systems. J. Aircraft, Nov-Dec, 1967.

4. Dempster, J.B. and Arnold, J.I.: Flight Test Evaluation of an Advanced Stability Augmentation System for the B-52 Aircraft. AIAA Paper No. 68-1068, Oct. 1968.

5. Roger, K.L. Hodges, G.E. and Felt, L.: Active Flutter Suppression - A Flight Test Demonstration. AIAA Paper No. 74-402, Apr. 1974.

6. Perisho, C.H., Triplett, W.E., and Mykytow, W.J.: Design Considerations for an Active Suppression System for Fighter Wing/Store Flutter. AGARD-CP-175, Apr. 1975.

7. Honlinger, H., and Lotze, A.: Active Suppression of Aircraft Flutter. To be presented at the ICAS Conference, Lisbon, Sept. 1978.

8. Wykes, J.H., and Mori, A.S.: Techniques and Results of an Analytical Investigation Into Controlling the Structural Modes of Flexible Aircraft. AIAA Symposium on Structural Dynamics and Aeroelasticity, Aug.-Sept. 1965.

9. Wykes, J.H. and Mori, A.S.: An Analysis of Flexible Aircraft Structure Mode Control. AFFDL-TR-65-190, Pt. I, U.S. Air Force, June 1966.

10. Topp, L.J.: Potential Performance Gains by Use of a Flutter Suppression System. Paper No. 7-B3, 1971 Joint Automatic Control Conference (St. Louis, Mo.), Aug. 1971.

11. Thompson, G.O., and Kass, G.J.: Active Flutter Suppression - An Emerging Technology, J. Aircraft Mar. 1972.

12. Many Authors: Impact of Active Control Technology on Airplane Design. AGARD CPP-157, Oct. 1974.

13. Many Authors: Active Control Systems for Load Alleviation, Flutter Suppression, and Rise Control. AGARD AG175, 1974.

14. Redd, L.T., Gilman, J., Jr., Cooley, D.E. and Sevart, F.D.: Wind-Tunnel Investigation of a B-52 Model Flutter Suppression System. J. Aircraft, Nov. 1974.

15. Sandford, M.C., Abel, I. and Gray, D.L.: Transonic Study of Active Flutter Suppression Based on an Energy Concept. NASA TR R450, Dec. 1975.

16. Nissim, E.: Flutter Suppression Using Active Controls Based on the Concept of Aerodynamic Energy. NASA TN D-6199, Mar. 1971.

17. Nissim, E.: Recent Advances in Aerodynamic Energy Concept for Flutter Suppression and Gust Alleviation Using Active Controls. NASA TN D-8519, Sept. 1977.

18. Garrick, I.E.: Perspectives in Aeroelasticity. Fifth Theodore von Karman Memorial Lecture. Israel Journal of Technology, 1972.

19. Nissim, E.: Flutter Suppression and Gust Alleviation Using Active Controls. TAE Rep. No. 198 - Technion, Israel Inst. Technol., 1974 (Available as NASA CR-138658).

20. Nissim, E., Caspi, A., and Lottati, I.: Application of the Aerodynamic Energy Concept to Flutter Suppression and Gust Alleviation by Use of Active Controls. NASA TN D-8212.

21. Nissim, E.: Active Flutter Suppression Using Trailing-Edge and Tab Control Surfaces. J. AIAA, June, 1976.

22. Nissim, E., and Abel, I.: Development and Application of an Optimization Procedure for Flutter Suppression Using Active Controls. NASA TP 1137, Feb. 1978.

23. Abel, I., Perry, B. III, and Murrow, H.N.: Synthesis of Active Controls for Flutter Suppression on a Flight Research Wing. AIAA Paper 77-1062, Guidance and Control Conference, Aug. 1977.

24. Nissim, E., and Lottati, I.: Active Controls for the Suppression of External Store Flutter in the YF-17 Flutter Model. Submitted for publication in J. Aircraft.

25. Nissim, E.: Comparative Study Between Two Different Flutter Suppression Systems. To be published in J. Aircraft.

26. Gregory, R.A., Ryneveld, A.D., and Imes, R.S.: SST Technology Follow-On Program - Phase II: A Low Speed Model Analysis and Demonstration of Active Control Systems for Rigid Body and Flexible Mode Stability. Report No. FAA - SS-73-18, June 1974.

27. Nissim, E.: Study of Active Control Systems for Application to Supersonic Cruise Aircraft To be published.

28. Edward, J.W., Breakwell, J.V. and Bryson, A.E. Jr.: Active Flutter Control Using Generalized Unsteady Aerodynamic Theory. AIAA Paper No. 77-1061 Guidance and Control Conference, Aug. 1977.

29. Schultz, D.G. and Melsa, J.L.: State Functions and Linear Control Systems. McGraw-Hill Book Co., 1967.

30. Turner, M.R.: Active Flutter Suppression. AGARD-CP-175, Apr. 1975.

31. Pinnamaneni, R. and Stearman, R.O.: Design and Analysis of Flutter Suppression Systems Through the Use of Active Controls. AFOSR-TR-75-0964, Jan. 1975.

* * *

Table 1: Summary of Calculated Flutter Characteristics of Drone Research Vehicle.

Mach number	Basic wing (No control)		Closed-loop			
			Classical		Energy	
	Dyn press kPa	Freq Hz	Dyn press kPa	Freq Hz	Dyn press kPa	Freq Hz
0.9	24.1	16.9	43.4	8.6	46.9	8.3
0.8	26.2	18.0	*NF	-	*NF	-
0.7	27.7	19.4	*NF	-	*NF	-

*No flutter to sea level dynamic pressure

Table 2: Description of the Three Wing/Store Configurations of YF-17

Config. / Description		A	B	C
Tip Launch. rail		Aim-9E(flex)	Empty	Empty
W.S.1.543 Pylon		Not instal.	Aim-7s(rig)	Aim-9E(rig)
W.S.1.052 Pylon		Aim-7(rig)	Not instal.	Not instal.
ω_{n1}	(HZ)	6.5377	5.1218	7.0099
ω_{n2}	"	11.0111	7.5891	11.9223
ω_{n3}	"	13.3887	14.5104	14.9007
ω_{n4}	"	15.9500	16.2730	25.5323
ω_{n5}	"	24.3176	36.8006	38.2069
ω_{n6}	"	38.2780	38.5456	41.3348
ω_{n7}	"	44.4797	43.0960	46.9919

$\omega_{n,i}$ natural frequency of the i^{th} elastic mode. (HZ).

Table 3: Summary of Results: Three wing/store configurations of YF-17 with activated outboard T.E. control using L.D.T.T.F. and V = 98 m/s

	Basic Wing (no control)		C L O S E D - L O O P							
STRUCT. DAMPING	g = 0		g = 0				g = 0.015		g = 0.03	
CONFIG.	Flutter Dyn. Press. kPa	Freq. rad/s	Flutter Dyn. Press. kPa	Freq. rad/s	Max* RMS Control Rate deg/s/m/s	Max* RMS Control Rotation deg/m/s	Max* RMS Control Rate deg/s/m/s	Max* RMS Control Rotation deg/m/s	Max* RMS Control Rate deg/s/m/s	Max* RMS Control Rotation deg/m/s
A	3.64	80	8.91	10	83	2.39	72	2.23	65	2.10
B	2.63	43	8.95 8.95	10 37	161	4.17	87	2.53	68	2.17
C	4.31	65	8.52	10	156	3.15	121	2.69	104	2.49

* Values relate to flights up to dyn. press. of 5.26 kPa

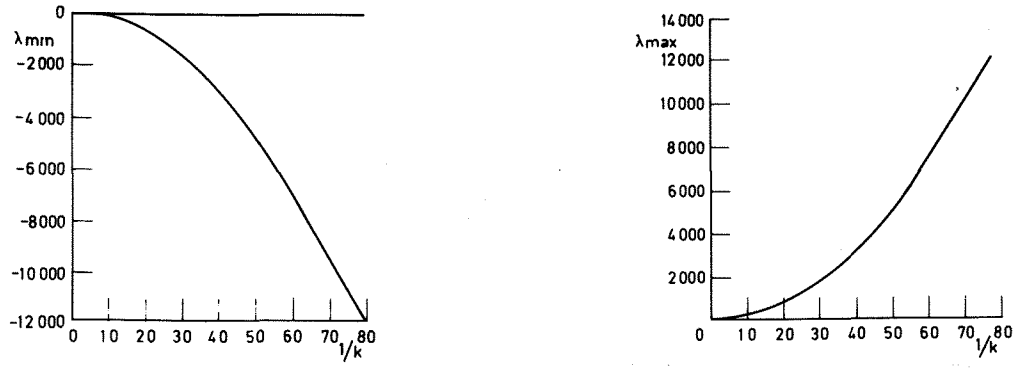

(a) λ_{min} (b) λ_{max}

Fig. 1. λ_{min} and λ_{max} vs 1/k. Wing strip with no control surfaces.

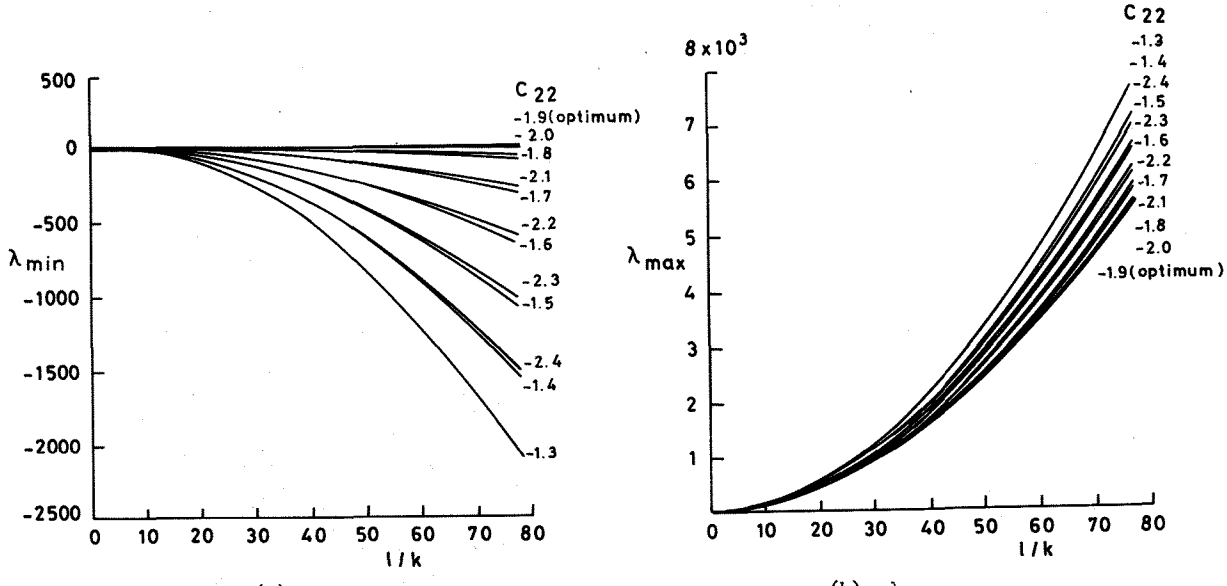

(a) λ_{min} (b) λ_{max}

Fig. 2. λ_{min} and λ_{max} vs 1/k for various values of C_{22}. Wing strip with T.E. control using eqns (11), (11a).

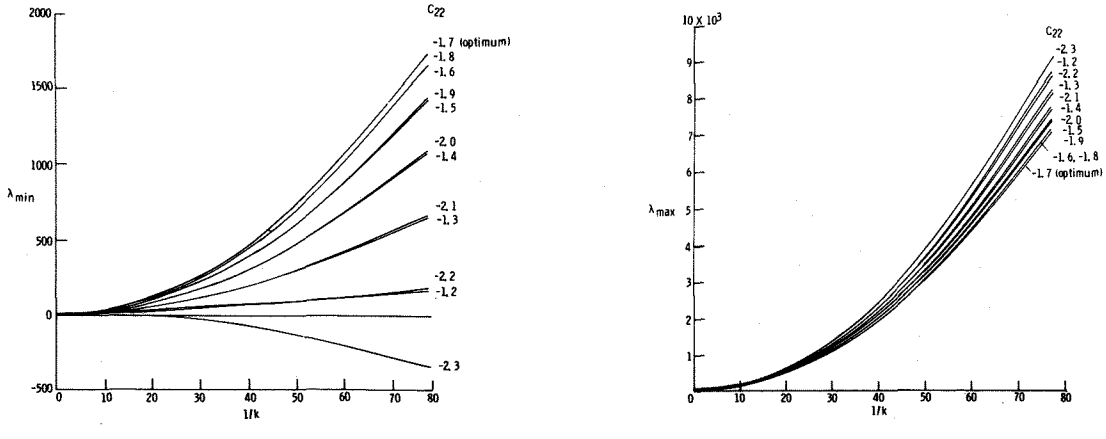

(a) λ_{min} (b) λ_{max}

Fig. 3. λ_{min} and λ_{max} vs 1/k for various values of C_{22}. Wing strip with L.E.-T.E. controls using eqns (11), (11b).

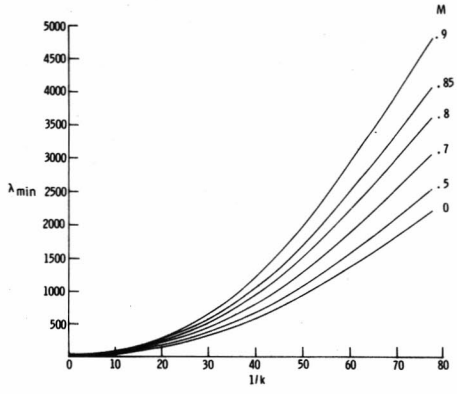

Fig. 4. λ_{min} vs 1/k at various Mach numbers. Wing strip with L.E.-T.E. controls using eqns (11), (11b).

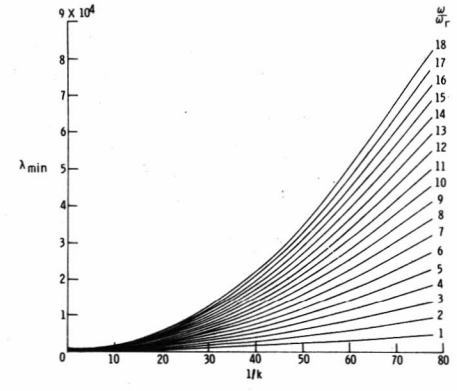

Fig. 5. λ_{min} vs 1/k for various values of ω/ω_r. Wing strip with L.E.-T.E. controls using eqns (11b), (12).

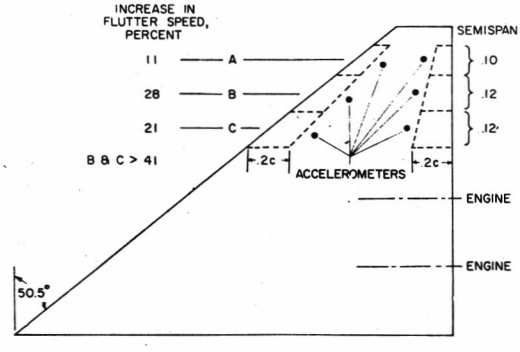

Fig. 6. Effectiveness of L.E.-T.E. system as flutter suppressor for SST type wing with engines.

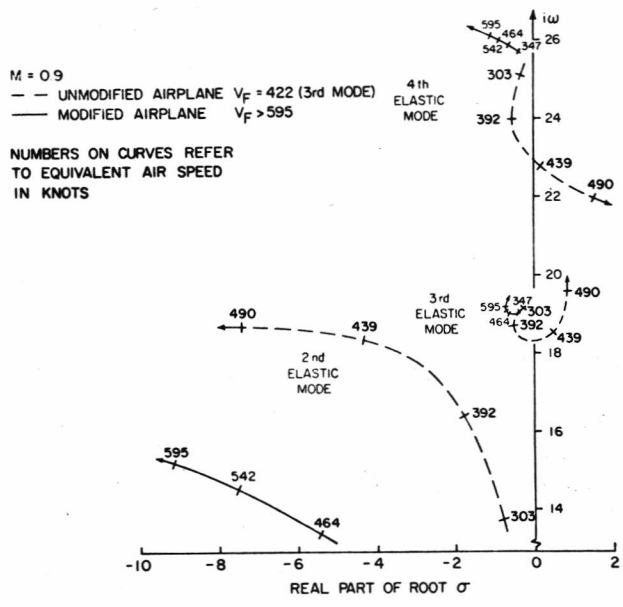

Fig. 7. Root locus plot comparing the unmodified airplane with modified one for combined case B and C of Fig. 6.

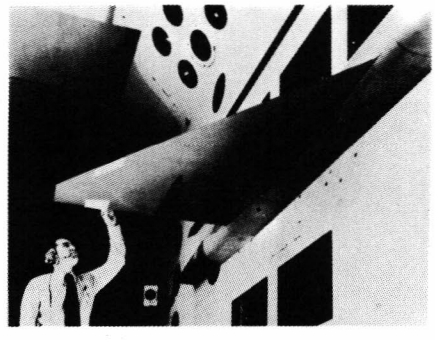

Fig. 8. Experimental wing for flutter suppression shown mounted in the Langley transonic dynamic tunnel.

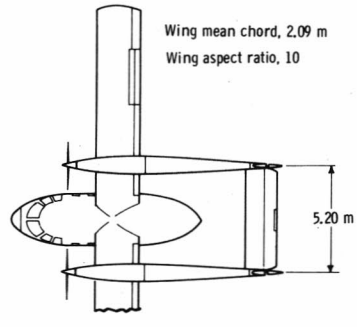

Fig. 9. Plan view of Arava STOL Transport.

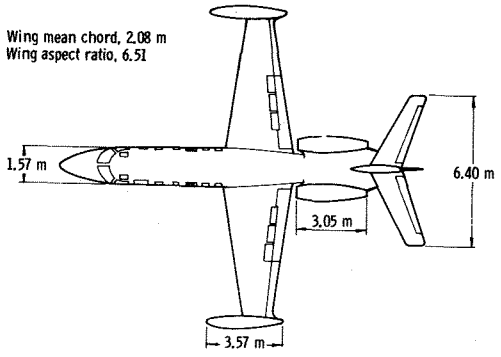

Fig. 10. Plan view of Westwind business jet transport.

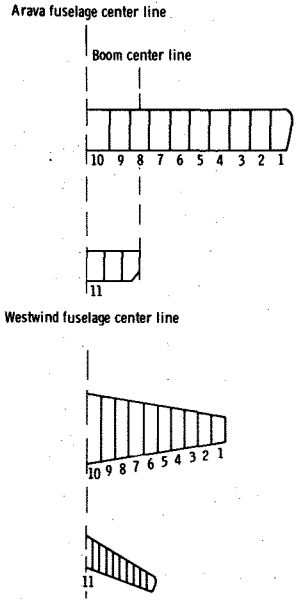

Fig. 11. Strip allocations along wing and horizontal tail of Arava and Westwind aircraft.

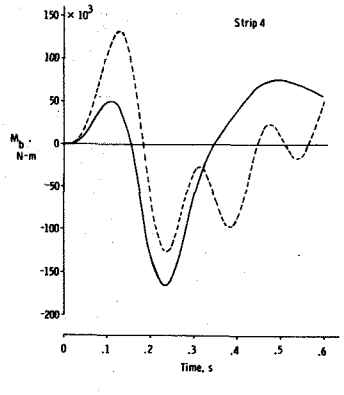

Fig. 12. Variation with time of wing root bending moment. Westwind transport with activated L.E.-T.E. system at strip 4 and with δ_{max}=0.5 rad.

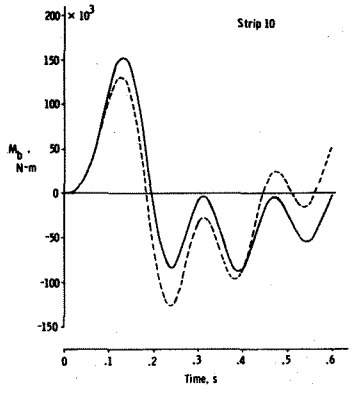

Fig. 13. Variation with time of wing root bending moment. Westwind transport with activated L.E.-T.E. system at strip 10 and with δ_{max}=0.5 rad.

----- without controls

——— with controls

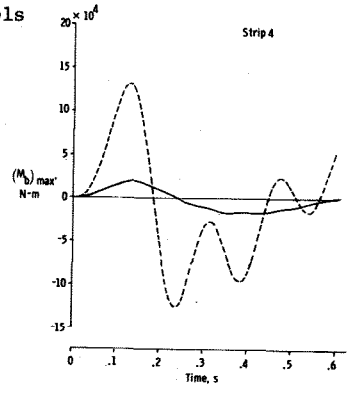

Fig. 14. Variation with time of wing root bending moment. Westwind transport with activated L.E.-T.E. system at strip 4 and with δ_{max}=0.5 rad. (using extended control law).

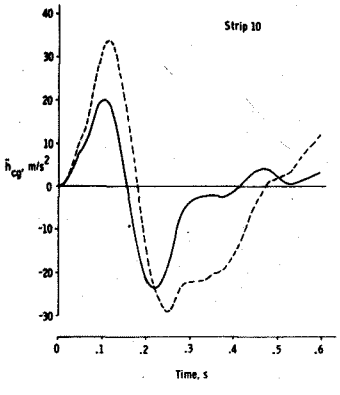

Fig. 15. Variation with time of linear acceleration at center of gravity. Westwind transport with activated L.E.-T.E. system at strip 10 and with δ_{max}=0.5 rad.

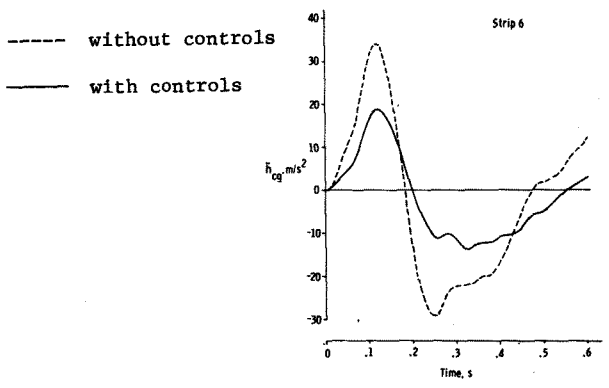

Fig. 16. Variation with time of linear acceleration at center of gravity. Westwind transport with activated L.E.-T.E. system at strip 6 and with δ_{max}=0.5 rad.(using extended control law).

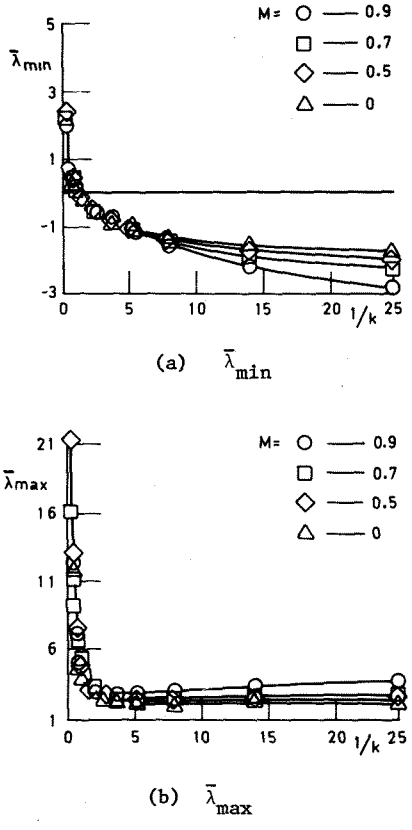

(a) $\bar{\lambda}_{min}$

(b) $\bar{\lambda}_{max}$

Fig. 17. $\bar{\lambda}_{min}$ and $\bar{\lambda}_{max}$ vs 1/k at various Mach numbers. Wing strip with no control surfaces.

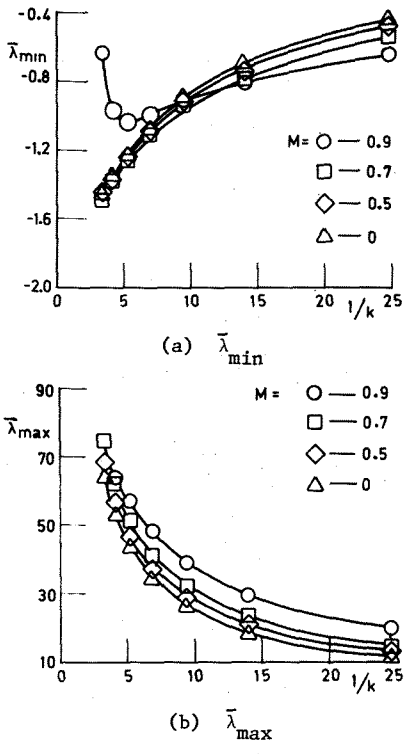

(a) $\bar{\lambda}_{min}$

(b) $\bar{\lambda}_{max}$

Fig. 18. $\bar{\lambda}_{min}$ and $\bar{\lambda}_{max}$ vs 1/k at various Mach numbers. Wing strip with T.E. control using D.T.T.F.

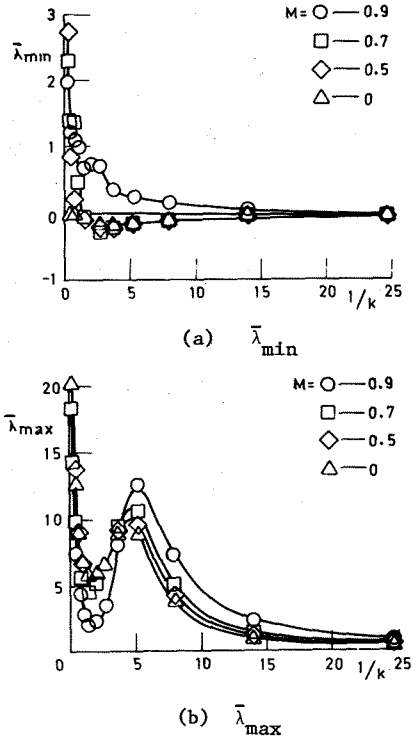

(a) $\bar{\lambda}_{min}$

(b) $\bar{\lambda}_{max}$

Fig. 19. $\bar{\lambda}_{min}$ and $\bar{\lambda}_{max}$ vs 1/k at various Mach numbers. Wing strip with T.E. control using L.D.T.T.F.

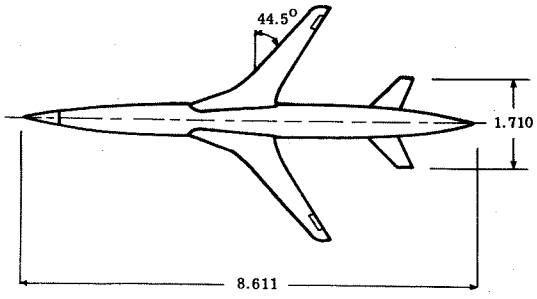

Fig. 20. Plan view of drone research vehicle (linear dimensions are in meters).

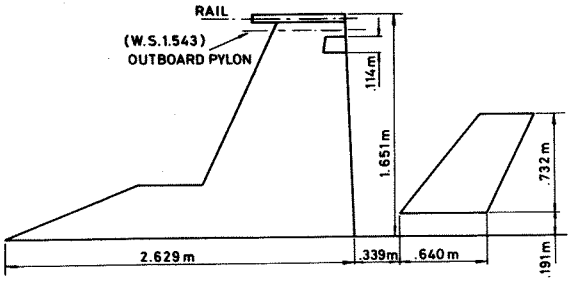

Fig. 23. Plan view (schematic) of YF-17 flutter model.

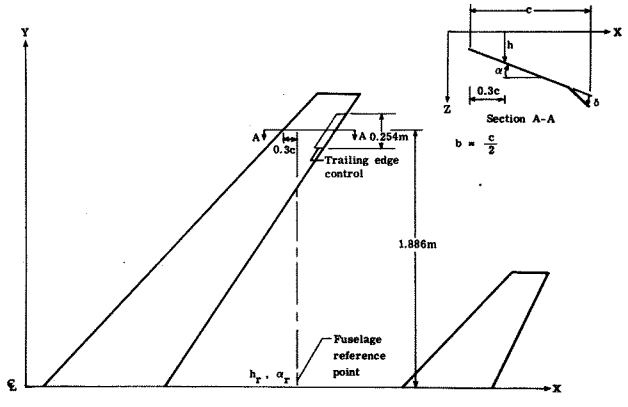

Fig. 21. Geometrical description of active control system for the drone vehicle.

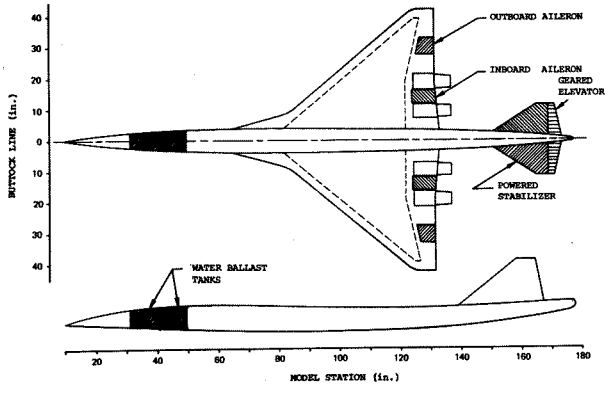

Fig. 24. General configuration of the SST model.

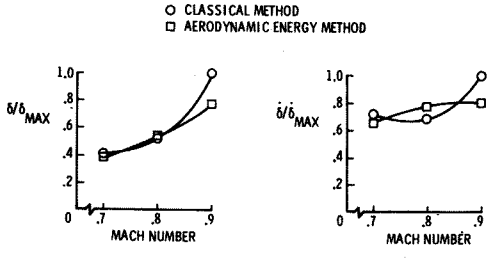

Fig. 22. Comparisons of control surface rates and displacements for the drone vehicle.

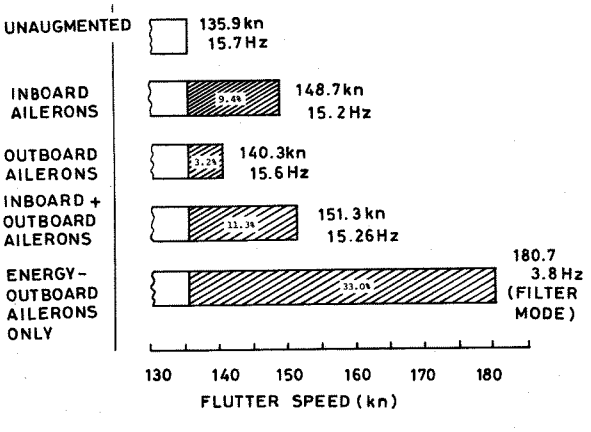

Fig. 25. Flutter results for the SST model.